Applied Surface Science 604 (2022) 154646

Contents lists available at ScienceDirect

Applied Surface Science

journal homepage: www.elsevier.com/locate/apsusc

Full Length Article

Semiconductive vertical graphene nanoribbons self-assembled on diamond (1 0 0) surface by oxidation: A DFT study

C.K. Chen [1], D.F. Guo [1], D. Fan [1], S.H. Lu, M.Y. Jiang, X. Li, X.J. Hu [*]

College of Materials Science and Engineering, Zhejiang University of Technology, Hangzhou 310014, PR China

ARTICLE INFO

Keywords:
Graphene nanoribbons
Diamond oxidation
First-principles calculations
Band structures

ABSTRACT

We predicted a self-assembly vertical zigzag graphene oxide nanoribbons (GONR) on diamond (1 0 0) surface using the structure swarm intelligence algorithm. The results show that the GONR surface structure is dynamically and thermally stable even applied by extra strains and high temperature of 2000 K. The GONR surface structure has unique chemical bonding including hexagonal sp^2-hybridized carbon sheets, C—O—C and C═O groups. Furthermore, GONR (width n = 1, 2, 3) surface structure exhibits a semiconductive and nonmagnetic properties with an indirect band gap, and it can be converted to semi-metals with magnetism when the width is greater than 3. The scanning tunneling microscopy image and Raman spectrum are also calculated, which give a characterization method for GONR in experiment. Our results supply a way to prepare semiconductive GONR structure by oxidizing diamond (1 0 0) surface and have an important significance in the development of graphene-based nano-electronic devices.

1. Introduction

Graphene has received much attention in recent years due to its technologically promising electronic properties [1], which have raised the possibility of using graphene in the next generation nano-electronics. However, the pristine graphene remains metallic even at the charge neutrality point and exhibits gapless property, dramatically hampering the development of graphene-based nano-electronic devices [2]. To overcome this problem, several mechanisms on modulating the band gap of graphene have been studied, including breaking symmetry by introducing impurity atoms [3–5], functionalization of graphene edges [6,7], and tailoring graphene nanoribbons (GNRs) through the control of their width and helicity. Especially, GNRs had been investigated for over two decades without exhausting their wonders and challenges, since their unique quantum confinement and edge physics predicted by first-principles calculations [8]. In contrast to semi-metallic graphene, GNRs typically possess a finite bandgap depending on their edge type and width [9,10], thus exhibiting attractive potential in future nano-electronics, spintronic, and quantum information technologies [11].

It was reported that pristine GNRs can be twisted or warped, causing its global mechanical instability, which can significantly influence the electronic and magnetic properties of free-standing GNRs [12–14]. Even though this mechanical deficiencies can be mitigated by introducing the substrate, the electronic structure and carrier mobility of GNRs will change due to the strongly interaction between π electrons and the substrates [15,16]. Experimentally, the vertically oriented graphene nanosheets (graphene nanowalls) had been demonstrated to improve the performances of GNRs, due to their unique orientation and huge surface-to-volume ratio [17–20]. By using radical injection plasma-enhanced chemical vapor deposition, Kondo et al. showed that O radical had a significant effect to improve the quality of vertically oriented nanowalls [21]. Unfortunately, these experimental results show that it is a big challenge to control the morphology of the vertically oriented graphene nanosheets on transition metal or other commonly substrates [22].

Yuan et al. reported that a unique vertical GNRs terminated by hydrogen was assembled on diamond (1 1 1) surface based on the first-principles calculations [23]. Due to the strong C—C σ bond between GNRs edge and substrates, the proposed configuration can significantly increase the dynamic stability, yet retaining the electronic, magnetic properties and high carrier mobility of defect-free GNRs. This suggests that using diamond as a substrate, GNRs have good stability and maintain excellent electrical properties. Also, we recently find that

* Corresponding author.
E-mail address: huxj@zjut.edu.cn (X.J. Hu).
[1] These authors contributed equally to this work.

https://doi.org/10.1016/j.apsusc.2022.154646
Received 30 April 2022; Received in revised form 10 August 2022; Accepted 21 August 2022
Available online 24 August 2022

vertical graphene nanosheets can directly grow on diamond in hydrogen and oxygen rich atmosphere by chemical vapor deposition [24]. However, how vertical graphene sheets grow on diamond is still an open question. Based on the results of hydrogen terminated GNRs assembled on diamond surface [23], it is interesting to know if oxygen plays role in the growth of vertical graphene sheets on diamond surface and give useful guidance for the experimental fabrication.

In this work, we report a self-assembly formation of vertical GNRs on oxidizing diamond (1 0 0) substrate by using theoretical calculations, called vertical zigzag graphene oxide nanoribbons (GONR) structure. The structure is dynamically and thermally stable, and it is robust against a certain degree of tensile strain and even a very high temperature. It is therefore possible to fabricate this surface structure experimentally by oxidizing diamond (1 0 0) surface. Also, our proposed surface system possesses tunable bandgaps controlled by the width of graphene nanoribbons. And the scanning tunneling microscopy image and Raman spectrum are calculated, giving a characterization method for GONR in experiment. Our results supply a way to prepare semiconductive GONR structure and have an important significance in the development of graphene-based nano-electronic devices.

2. Method

Our structural searches of the oxidized diamond (1 0 0) surface with simulation cell sizes of up to 20 atoms were performed in the CALYPSO code [25]. Previous found surface structures are further relaxed within the framework of DFT as implemented by VASP (Vienna Ab initio Simulation Package) code [26]. Both hydrogen passivation and symmetric slabs are used to model oxidized diamond (1 0 0) surface. 9 and 14 monolayers of C atoms are used in hydrogen passivation and symmetric slabs, respectively. 25 Å vacuum region along z-direction has been placed to avoid the direct interaction between the bottom and top surface. Generalized gradient approximation with the Perdew–Burke–Ernzerhof (PBE) functional [27] and projector augmented wave (PAW) potentials [28] are adopted in DFT calculations. A $3 \times 3 \times 1$ Monkhorst-pack grid is used to sample the Brillouin zone and the plane wave cut off energy is set to 900 eV. The positions of atoms are allowed to relaxed with converged gradient method until the forces are less than 0.01 eV/Å, and the energy converges to 10^{-5} eV. The van der Waals Density Functional (vdW-DF) method was included in our calculations to describe weak interlayer interaction [29–31]. Heyd–Scuseria–Ernzerhof (HSE06) functional [32] is used to obtain the accurate band structures. To study the dynamic and thermal stability of the proposed structures, we perform ab initio phonon calculations by direct supercell method as implemented in PHONOPY code [33] and ab initio molecular dynamics (AIMD) simulations using the canonical ensemble.

To evaluate the relative stability of the candidate surface structures with different number of surface atoms, we define the surface formation energy ΔE as

$$\Delta E = E_{tot}^{surf} - n\mu_c - m\mu_0, \quad (1)$$

Where E_{tot}^{surf} is the total energy of the simulated slab, n and m represent the number of carbon and atoms in the systems, μ_c and μ_0 are the chemical potentials C and O atoms, respectively. μ_c is set to the bulk energy as the system is assumed to be in chemical equilibrium with bulk diamond [34].

3. Results and discussion

3.1. GONR surface structures

Fig. 1a shows the relaxed structure of GONR with unique chemical bonds. For comparison, the previously proposed ketone and ether

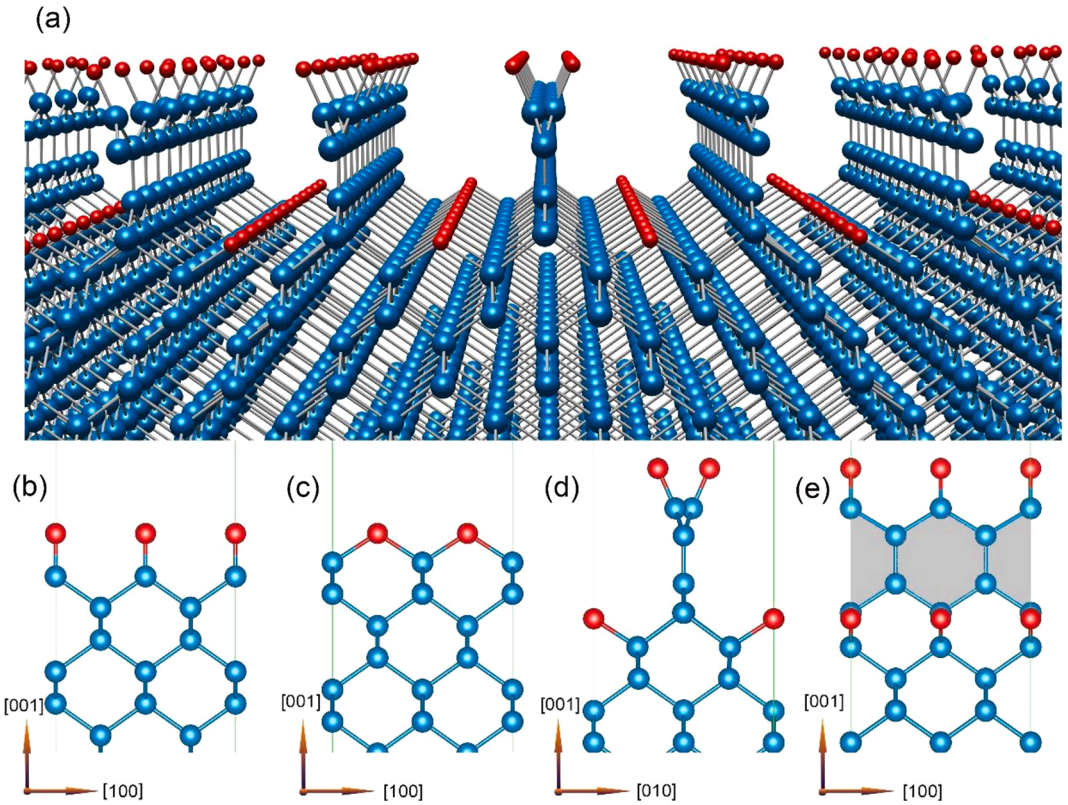

Fig. 1. Schematic drawing of relaxed configurations oxidized diamond (1 0 0) surfaces: (a) three-dimensional structure diagram of GONR, two-dimensional structure diagram of (b) [1 0 0] directional Ketone (c) [1 0 0] directional ether, (d) [0 1 0] directional GONR (e) [1 0 0] directional GONR. Color code: red, oxygen atoms; cyan, carbon atoms.

structures [35] are also illustrated in Fig. 1b and 1c, respectively. Our DFT calculation indicates that the formation energy of GONR surface structure is significantly lower than the reported most stable ether surface by 0.138 eV per (1 × 1) unit cell *via* PBE functional [35]. Besides the well accepted PBE functional, various functionals have also been used to examine the structures relative stability and they produce similar results (Table S1).

As shown in Fig. 1a, the GONR surface structure contains various bonding types, including hexagonal sp^2-hybridized carbon sheets, C—O—C and C═O groups. And its corresponding planar structure in two different directions of [0 1 0] and [1 0 0] is shown in Fig. 1d and 1e. This unique structure is composed of diamond substrate, the (1 0 0) surface terminated by O atoms partially as an ether structure (C—O—C, 1.46 Å), and a hexagonal carbon lattice, in which the bottom side of the edges (closely resembles zigzag-edge graphene nanoribbon, GNR) is tightly binding on the diamond (1 0 0) surface by strong C—C σ bonds. Besides, the top side of the GNR edge is terminated via C═O bonds (1.22 Å). Moreover, our first-principles calculations show that the oxygen atoms fluctuation of left and right position exhibit a lower formation energy compares with linear structure.

Motivated by atomic self-assembly GONR surface structure and the recent experimental and theoretical researches in graphene-based materials, we design a kind of diamond-supported vertical zigzag GONR (see Fig. S1) *via* adding hexagonal carbon lattices. Unlike epitaxial graphene sheets on metal or insulating substrates, which lies flat on the substrate, and bonded via weak van der Waals forces [29–31], this type of newly proposed GONR(n) surface structures completely bonds with diamond (1 0 0) surface by a strong C—C covalent bond. Interestingly, with the increase of nanoribbons width on the diamond substrate, the geometric configurations of the edge states transform from the regular oscillation to completely straightened structure when n > 3 (see the detailed structural diagrams in Fig. S1). This nonreversible transmutation is controlled by the increased π–π interaction between two parallel graphene oxide nanowalls.

3.2. Energetic, kinetic, and thermal stability of GONR surface structure

Total energy calculations based on DFT show that the newly predicted GONR surface is significantly more stable than previous known ketone and ether surface structures. The pristine DFT theory cannot describe weak van der Waals force, so we further adopt vdw-DF2 [31] and revPBE-vdw [36] to explicitly add vdW corrections in the total energy calculations (see Table S2). Though different correction methods give slightly different energy differences, both functionals give the same results: GONR structure is more stable than ketone and ether surfaces. The additional energetic advantage of forming GONR on diamond surfaces is reflected in the negative formation energy with respect to ketone and ether structures. Fig. 2a demonstrates the calculated formation energy of different terminated diamond (1 0 0) surface as a function of oxygen chemical potential. As can be seen, GONR has lower energy

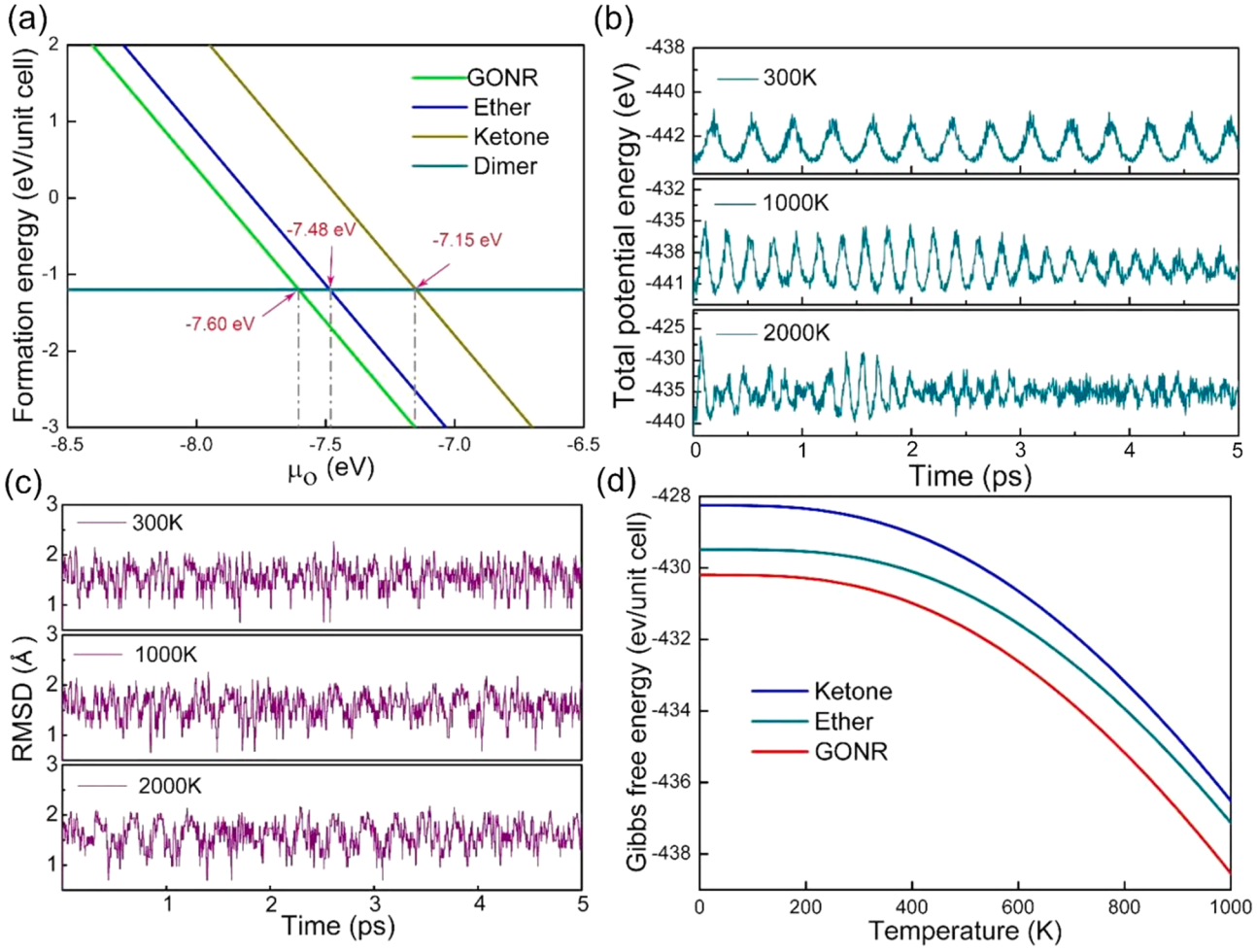

Fig. 2. Stability of GONR surface structure. (a) Calculated formation energy of diamond (1 0 0) surface with different surface terminations. Dimer is the reconstructed diamond (1 0 0) surface. (b) Evolution of potential energy of GONR during AIMD simulations at 300 K, 1000 K, 2000 K, respectively. (c) Plot of RMSD traces show the stability of GONR surface structure as a function of simulation time. (d) The Gibbs free energy within PBE functional of GONR structure with respect to ketone and ether surface structure as a function of temperature.

formation than that of ether and ketone in whole range of oxygen chemical potential. And the position of the intersection represents the oxygen chemical potential needed to form the corresponding structure. As oxygen chemical potential decreases to −7.60 eV, it becomes energetically favorable to form GONR on diamond (1 0 0) surface, while the oxygen chemical potential decreases to −7.48 eV and −7.15 eV, it prefers to form Ether and Ketone, respectively.

Next, we studied the thermal stability of GONR structure by performing AIMD at different temperatures. Fig. 2b summarizes the evolution of potential energy of GONR surface structure at 300 K, 1000 K and 2000 K for 5 picoseconds with a time step of 1 fs during AIMD simulations. As shown in AIMD dynamics curve of these temperatures, the total potential energy fluctuates up and down in a straight line, which indicates that the GONR structure is very stable. Furthermore, structural stability of GONR surface is checked by analyzing the backbone root-mean-square deviation (RMSD) from the starting crystal configuration over the process of the trajectory, as shown in Fig. 2c. It is evident that the RMSD levels stay around 1.5 Å over the entire length of simulation time at different temperatures, indicating that the geometric configuration is expected to be very stable. These results have demonstrated that the thermal stability of GONR surface structure is robust.

The relative energetic stability of the GONR structures can be further confirmed by external perturbations, such as compressive strain or elevated temperatures. The effects of external strain on the stability of various structures are demonstrated in Fig. S2. We examine the formation energy of ketone, ether and GONR surface structures under three typical strains (uniaxial [1 0 0] and [0 1 0], and biaxial), respectively. One can notice that the tendency of the formation energy shows a similarity with the strain imposed along the different crystallographic directions, but the GONR surface structure also has a low formation energy comparing with other two configurations. Especially, 4 % is the global minimum of the formation energy when we perform a tensile stress test along the [0 1 0] direction, demonstrating that the GONR surface configuration prefers to exist and has an outstanding stability. This significant effect of strains on the structural stability provides a profitably guidance for the synthesis of GONR surface structure in experiment.

To evaluate the effects of temperature on the stability of the GONR surface structure, the variation tendency of Gibbs free energies as a function of the temperature were demonstrated (as depicted in Fig. 2d). It is found that GONR surface structure is energetically in favor of 0 K, which Gibbs free energy is lower by 1.24 eV/unit cell than ether surface structure. Furthermore, comparing with ether surface structure, we find that the GONR surface structure also has a lower Gibbs free energy with the increase of the temperature, reaching 1.42 eV/unit cell at 1,000 K. Next, the lattice dynamic stability is further confirmed by calculating the phonon dispersion spectrum of the GONR surface structure, as shown in Fig. S3. The absence of imaginary modes in the entire Brillouin zone

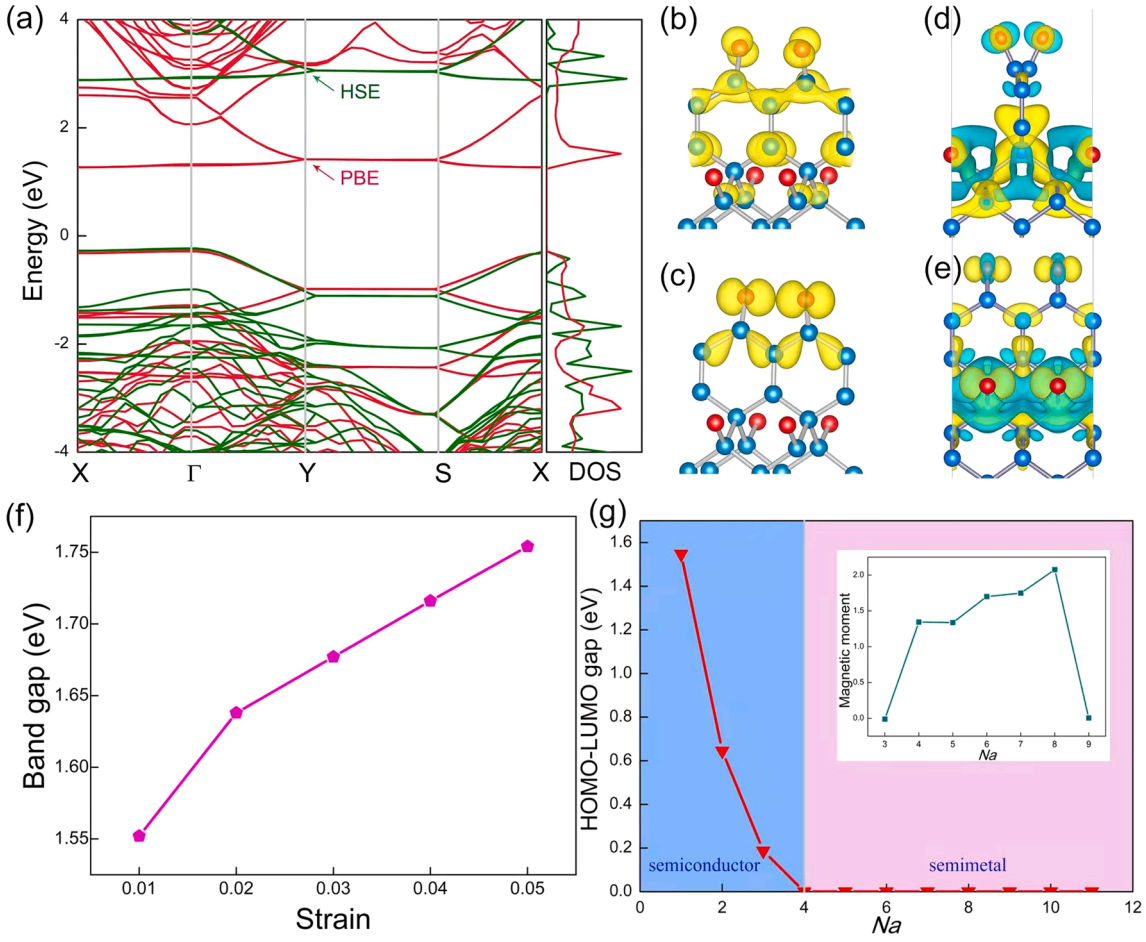

Fig. 3. Electronic properties (a) Band structure, using PBE (red line) and HSE (green line) functional which fermi level is shifted to 0 eV, and band-decomposed Charge densities of CBM and VBM at the X, gamma point for (b) and (c), respectively. (d) and (e) represents the 3D differential electronic density map (along the different perspectives), in which the yellow and green colored volumes represent the charge accumulation and depletion, respectively. The isosurface correspond to 0.034 eV/Å^3 (f) A plot of band structures of the GONR surface structure versus the tensile strain, varying from 1 % to 5 %. The tensile strain has a significant effect on the electronic properties of the surface structure. (g) HOMO-LUMO gaps of GONR surfaces structure as a function of ribbon width *Na*. The illustration shows the magnetic moment (in units of μm) of the ferromagnetic state as a function of ribbon width *Na*. (For interpretation of the references to color in this figure legend, the reader is referred to the web version of this article.)

confirms that the structure is dynamically stable and remarkable phonon gap is observed in the phonon spectra. We find that not only the GONR surface structure is dynamically robust but also it is thermally stable at high temperatures (up to 2000 K).

3.3. Electronic structures

Fig. 3 shows the band structures of GONR surface structure and corresponding band decomposed charge densities. It is observed that the valance band maximum (VBM) lies on the Γ point whereas the conduction band minimum (CBM) is located at the X point, indicating the GONR surface structure is an indirect band-gap semiconductor. The calculated band gap is 1.55 eV by the PBE functional, while a more accurate prediction using the hybrid HSE06 functional is 3.10 eV. The detailed analyses of Bader charge analysis are given in Table S3. It indicates that both the valence band and the conducting band are originated from oxide nanoribbons and the electronic states near the fermi level primarily caused by the O atoms on the edges and the sp^2 hybridized C atoms, confirmed by the band decomposed charge density distributions and 3D differential electronic density (see b, c and d, e in Fig. 3, respectively). The electron localization function (ELF) is used to understand the unique bonding characteristics (see Fig. S4). A basin of electron localization is found between the C atoms in nanoribbons, indicating the formation of covalent bonds between them. The C atoms are sp^2 hybridized and include both σ and π bonds with their neighboring C atoms. This unique bonding type makes the unusual bonds characteristics comparing with the C—C distances in graphene (1.42 Å).

Moreover, we investigate the effects of tensile strains on the electronic properties of GONR surface structure. The results show that the strains along different directions have a clearly influence on the band structures (see Fig. 3f for strain-dependent band structures). As a result, we can see the band gap of GONR surface structure exhibits a linear response to the tensile strain ranging from 1 % to 5 %. This interdependence means that one can tune band gap efficiently by bringing suitably tensile strains to bear on GONR surface structure. Also, our band structure results show that the modification of band gap for the VBM slight movement is arising from the C═O bonding states, but the CBM is mainly contributed by all atoms in nanoribbons, so the tensile strain has much less effect on the VBM.

It was reported that graphene nanoribbons with homogeneous armchair or zigzag shaped edges all have energy gaps which decreases as the width of the system increase [37]. Armchair GNRs present a metallic, nonmagnetic and not apparent effect by regardless of the width of nanoribbons, while the GNRs with zigzag shaped edges, their band gaps are originated from a staggered sublattice potential due to spin ordered states at the edges [38–40]. Also, zigzag-edged GNRs with precisely-tunable π-magnetism hold great potential for applications in spintronics and quantum devices [41–43]. Particularly, the properties of half-metallicity in edge-oxidized zigzag graphene nanoribbons has been reported and spin magnetization rapid decrease with the increase of the external electric field, eventually systems reached nonmagnetic [9]. Therefore, we explore the band gap behavior of the GONR on the diamond (1 0 0) substrate. Our calculations demonstrate that the ground state of GONR (n = 1, 2, 3) is nonmagnetic, while the ground state of other structures (n > 3) is magnetic which exhibit very different characteristics from zigzag GNRs in the previous reports. In Fig. 3g, the HOMO-LUMO gap oscillations as a function of the ribbon width and this periodicity of the oscillation appears to be significantly different from the previously reported zigzag graphene nanoribbons [37,39,44]. It indicates that GONR (n = 1, 2, 3) show a semiconductive property and GONR (n) can be converted to semi-metals as long as the width greater than 3. And also, maybe, the half-metallicity in nano-scale GONR structures can be tuned by external electric fields or appropriate chemical edge modifications [45,46]. The spin polarization and giant magnetoresistance in GONR surface structure also can be realized, so this alternative device based GONR can be applied as a spin filter probably [47,48]. These hierarchies are different from the armchair GNRs or free-standing GNRs on substrates during to its amazing bonding features. We consider that these completely different electronic properties are originated from the unique surface nanoribbons configuration, in which one of the edges is terminated by O atoms, while the other edge is bound to diamond substrate (is covered by C—O bridges partially) tightly.

Meanwhile, in order to further analyze the electron orbital contribution of each atom, we calculated the total density of states (TDOS) and the partial density of states (PDOS) of GONR surface structure. As shown in Fig. 4, the peak position and intensity of electron state density of O1 (at the edge of GONR) and O3 (on the diamond (1 0 0) surface) have a great change in the energy range of −8–8 eV. This reflects the difference bonding type with ketone and *sp3* bonded ether structures.

In addition, the contribution of the electron density of states to the p-orbitals of the C atoms in the energy range of $-8 \sim 8$ eV is also quite different under the action of the oxygen surface states. As can be seen, the PDOS of the C1 and O1 atoms have multiple resonance peaks in the energy range, indicating the formation of a strong C═O bonding. Compared with the C1 atom, the p-orbitals contribution of C3 and C6 has obvious changes in the position and intensity below the Fermi level, mainly the p_x-orbital contribution. And the contribution of s, p_y and p_z-orbitals of C7 and C9 to the electron density increases significantly, which is caused by the surface state of oxygen.

3.4. Characterization of GONR surface structure

The theory for simulating scanning tunneling microscopy (STM) imaging by ab initio density functional calculations has been well established [49]. To identify the formation characteristics of the GONR surface structure, we simulated its STM with a tip bias of + 0.1 V shown in Fig. 5. It is observed that the surface atomic arrangement structure of GONR is obviously different from that of ketone and ether.

Moreover, we calculated the Raman spectra and electron affinity (EA) of ketone, ether and GONR surface structures based on the DFT methods (shown in Fig. S5). The GONR surface structure has quite a lot of Raman active and an extremely significant different active at 1660 cm^{-1} and 1748 cm^{-1} peak (C═C stretching vibration frequency and C═O groups, respectively). For ether surface structure, its EA is estimated to be + 1.4 eV which is close to the experimental results (1.0–1.7 eV) [50], while the EA of GONR surface structure is even greater (reached + 2.9 eV). The result suggests that oxygen plays a key role in the direct growth of vertical graphene sheets on diamond surface, confirmed by our recent experimental results [24]. And more meaningful, the previous experimental results show that the orientation and nucleation of GNRs on the substrates strongly depend on the addition of O_2 gas [21]. Hence, we believe that it is possible to synthesize this specific type of GONR structure in highly ordered and at very low cost.

4. Summary

In summary, by using the structure swarm intelligence algorithm combined with DFT calculations, a self-assembly vertical zigzag GONR on diamond (1 0 0) surface is predicted in this work. A series of theoretical calculations were performed and the results affirmed that GONR surface structure is dynamically and thermally stable even under applied extra strain or under high temperature of 2,000 K. And it has unique chemical bonding with hexagonal sp^2-hybridized carbon sheets, C—O—C and C═O groups owing to its special surface geometric configuration. The results show that GONR (width n = 1, 2, 3) exhibits indirect bandgap semiconductor and non-magnetic properties, and can be converted into semi-metals with magnetism when n > 3. Our results provide a way to prepare semi-conductive GONR structure and have an important significance for the development of graphene-based nanoelectronic devices.

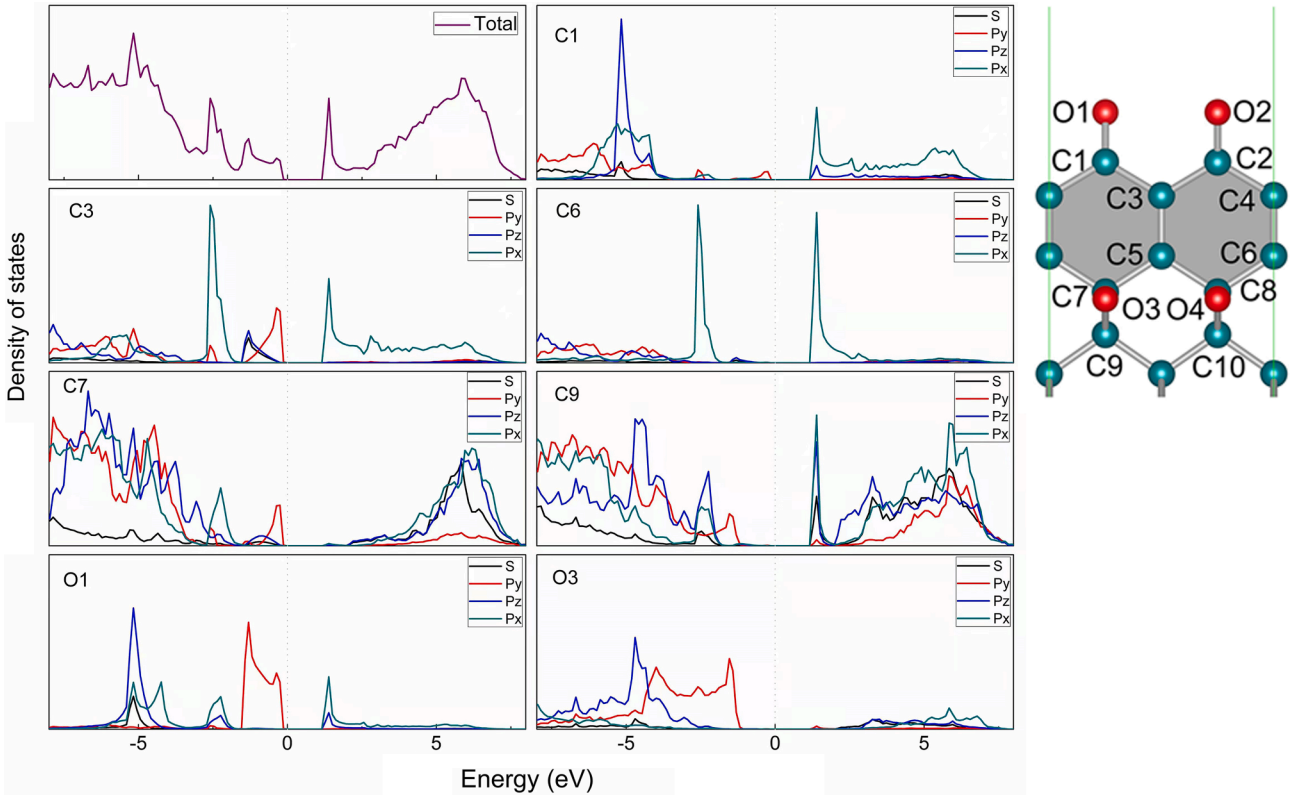

Fig. 4. TDOS and PDOSs of GONR surface structure. The DOS spectra are aligned such that the bulk VBM is at zero, as with the band structures.

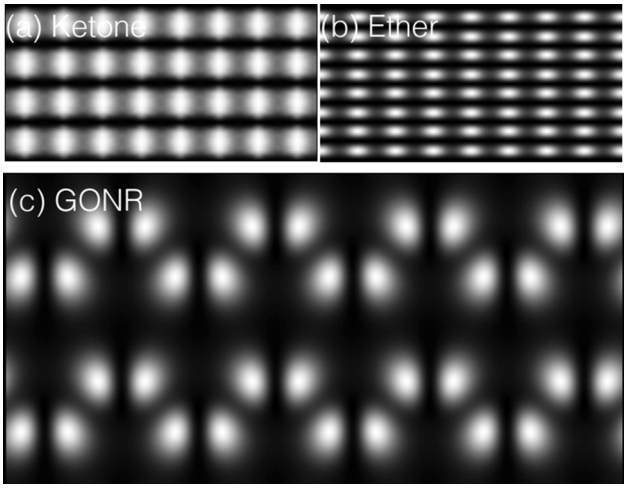

Fig. 5. Simulated scanning tunneling microscopy (STM) images of (a) ketone, (b) ether and (c)GONR surface structure with a tip bias of +0.1 V as shown in a top view.

CRediT authorship contribution statement

C.K. Chen: Investigation, Data curation, Visualization, Writing – original draft. **D.F. Guo:** Investigation, Formal analysis, Data curation. **D. Fan:** Formal analysis, Writing – original draft. **S.H. Lu:** Validation. **M. Y. Jiang:** Writing – review & editing. **X. Li:** Writing – review & editing. **X.J. Hu:** Funding acquisition, Conceptualization, Supervision, Writing – review & editing.

Declaration of Competing Interest

The authors declare that they have no known competing financial interests or personal relationships that could have appeared to influence the work reported in this paper.

Data availability

Data will be made available on request.

Acknowledgements

Key Project of National Natural Science Foundation of China (Grant No. U1809210) and National Natural Science Foundation of China (Grant Nos. 52102052, 50972129 and 50602039); Key Research and Development Program of Zhejiang Province (2018C04021); International Science Technology Cooperation Program of China (2014DFR51160); National Key Research and Development Program of China (No. 2016YFE0133200); European Union's Horizon 2020 Research and Innovation Staff Exchange (RISE) Scheme (No. 734578).

Data Availability

The data that support the findings of this study are available within the article and its supplementary material.

Appendix A. Supplementary material

Supplementary data to this article can be found online at https://doi.org/10.1016/j.apsusc.2022.154646.

References

[1] A.H. Castro Neto, F. Guinea, N.M.R. Peres, K.S. Novoselov, A.K. Geim, The electronic properties of graphene, Rev. Mod. Phys. 81 (2009) 109–162.

[2] K.S. Novoselov, A.K. Geim, S.V. Morozov, D. Jiang, M.I. Katsnelson, I. V. Grigorieva, S.V. Dubonos, A.A. Firsov, Two-dimensional gas of massless Dirac fermions in graphene, Nature 438 (2005) 197–200.
[3] T. Ohta, A. Bostwick, T. Seyller, K. Horn, E. Rotenberg, Controlling the electronic structure of bilayer graphene, Science 313 (2006) 951–954.
[4] Y. Zhang, T.T. Tang, C. Girit, Z. Hao, M.C. Martin, A. Zettl, M.F. Crommie, Y. R. Shen, F. Wang, Direct observation of a widely tunable bandgap in bilayer graphene, Nature 459 (2009) 820–823.
[5] I. Zanella, S. Guerini, S.B. Fagan, J. Mendes Filho, A.G. Souza Filho, Chemical doping-induced gap opening and spin polarization in graphene, Phys. Rev. B. 77 (2008), 073404.
[6] D.C. Elias, R.R. Nair, T.M.G. Mohiuddin, S.V. Morozov, P. Blake, M.P. Halsall, A. C. Ferrari, D.W. Boukhvalov, M.I. Katsnelson, A.K. Geim, K.S. Novoselov, Control of graphene's properties by reversible hydrogenation: evidence for graphane, Science 323 (2009) 610–613.
[7] T.O. Wehling, K.S. Novoselov, S.V. Morozov, E.E. Vdovin, M.I. Katsnelson, A. K. Geim, A.I. Lichtenstein, Molecular doping of graphene, Nano Lett. 8 (2008) 173–177.
[8] M. Fujita, K. Wakabayashi, K. Nakada, K. Kusakabe, Peculiar localized state at zigzag graphite edge, J. Phys. Soc. Jpn. 65 (1996) 1920–1923.
[9] O. Hod, V. Barone, J.E. Peralta, G.E. Scuseria, Enhanced half-metallicity in edge-oxidized zigzag graphene nanoribbons, Nano Lett. 7 (2007) 2295–2299.
[10] L. Yang, C.H. Park, Y.W. Son, M.L. Cohen, S.G. Louie, Quasiparticle energies and band gaps in graphene nanoribbons, Phys. Rev. Lett. 99 (2007), 186801.
[11] H. Wang, H.S. Wang, C. Ma, L. Chen, C. Jiang, C. Chen, X. Xie, A.P. Li, X. Wang, Graphene nanoribbons for quantum electronics, Nat. Rev. Phys. 3 (2021) 791–802.
[12] J.C. Meyer, A.K. Geim, M.I. Katsnelson, K.S. Novoselov, T.J. Booth, S. Roth, The structure of suspended graphene sheets, Nature 446 (2007) 60–63.
[13] V.B. Shenoy, C.D. Reddy, A. Ramasubramaniam, Y.W. Zhang, Edge-stress-induced warping of graphene sheets and nanoribbons, Phys. Rev. Lett. 101 (2008), 245501.
[14] K.V. Bets, B.I. Yakobson, Spontaneous twist and intrinsic instabilities of pristine graphene nanoribbons, Nano Res. 2 (2009) 161–166.
[15] C. Riedl, C. Coletti, T. Iwasaki, A.A. Zakharov, U. Starke, Quasi-Free-Standing Epitaxial graphene on SiC obtained by hydrogen intercalation, Phys. Rev. Lett. 103 (2009), 246804.
[16] S.Y. Zhou, G.H. Gweon, A.V. Fedorov, P.N. First, W.A.D. Heer, D.H. Lee, F. Guinea, A.H. Castro Neto, A. Lanzara, Erratum: Substrate-induced bandgap opening in epitaxial graphene, Nature Mater. 6 (2007) 916.
[17] K. Teii, S. Shimada, M. Nakashima, A.T.H. Chuang, Synthesis and electrical characterization of n-type carbon nanowalls, J. Appl. Phys. 106 (2009), 084303.
[18] J.J. Wang, M.Y. Zhu, R.A. Outlaw, X. Zhao, D.M. Manos, B.C. Holloway, V. P. Mammana, Free-standing subnanometer graphite sheets, Appl. Phys. Lett. 85 (2004) 1265–1267.
[19] M. Hiramatsu, K. Shiji, H. Amano, M. Hori, Fabrication of vertically aligned carbon nanowalls using capacitively coupled plasma-enhanced chemical vapor deposition assisted by hydrogen radical injection, Appl. Phys. Lett. 84 (2004) 4708–4710.
[20] Z. Bo, Z. Wen, H. Kim, G. Lu, K. Yu, J. Chen, One-step fabrication and capacitive behavior of electrochemical double layer capacitor electrodes using vertically-oriented graphene directly grown on metal, Carbon 50 (2012) 4379–4387.
[21] S. Kondo, S. Kawai, W. Takeuchi, K. Yamakawa, S. Den, H. Kano, M. Hiramatsu, M. Hori, Initial growth process of carbon nanowalls synthesized by radical injection plasma-enhanced chemical vapor deposition, J. Appl. Phys. 106 (2009), 094302.
[22] Z. Bo, Y. Yang, J. Chen, K. Yu, J. Yan, K. Cen, Plasma-enhanced chemical vapor deposition synthesis of vertically oriented graphene nanosheets, Nanoscale 5 (2013) 5180.
[23] Q. Yuan, H. Hu, J. Gao, F. Ding, Z. Liu, B.I. Yakobson, Upright standing graphene formation on substrates, J. Am. Chem. Soc. 133 (2011) 16072–16079.
[24] M.Y. Jiang, C.K. Chen, P. Wang, D.F. Guo, S.J. Han, X. Li, S.H. Lu, X.J. Hu, Diamond formation mechanism in chemical vapor deposition, PNAS 119 (2022) 2201451119.
[25] Y. Wang, J. Lv, L. Zhu, Y. Ma, CALYPSO: A method for crystal structure prediction, Comput. Phys. Commun. 183 (2012) 2063–2070.
[26] G. Kresse, J. Furthmüller, Efficient iterative schemes for ab initio total-energy calculations using a plane-wave basis set, Phys. Rev. B. 54 (1996) 11169–11186.
[27] J.P. Perdew, K. Burke, M. Ernzerhof, Generalized gradient approximation made simple, Phys. Rev. Lett. 77 (1996) 3865–3868.
[28] P.E. Blöchl, Projector augmented-wave method, Phys. Rev. B. 50 (1994) 17953–17979.
[29] M. Dion, H. Rydberg, E. Schröder, D.C. Langreth, B.I. Lundqvist, Van der Waals Density functional for general geometries, Phys. Rev. Lett. 92 (2004), 246401.
[30] G. Román-Pérez, J.M. Soler, Efficient implementation of a van der Waals density functional: application to double-wall carbon nanotubes, Phys. Rev. Lett. 103 (2009), 096102.
[31] J. Klimeš, D.R. Bowler, A. Michaelides, Van der Waals density functionals applied to solids, Phys. Rev. B. 83 (2011), 195131.
[32] J. Heyd, G.E. Scuseria, M. Ernzerhof, Erratum: "Hybrid functionals based on a screened Coulomb potential" [J. Chem. Phys. 118, 8207 (2003)], J. Chem. Phys. 124 (2006) 219906.
[33] A. Togo, F. Oba, I. Tanaka, First-principles calculations of the ferroelastic transition between rutile-type and $CaCl_2$-type SiO_2 at high pressures, Phys. Rev. B. 78 (2008), 134106.
[34] Y. Yu, C.Z. Gu, L.F. Xu, S.B. Zhang, Ab initio structural characterization of a hydrogen-covered diamond (001) surface, Phys. Rev. B. 70 (2004), 125423.
[35] S.J. Sque, R. Jones, P.R. Briddon, Structure, electronics, and interaction of hydrogen and oxygen on diamond surfaces, Phys. Rev. B. 73 (2006), 085313.
[36] A. Gulans, M.J. Puska, R.M. Nieminen, Linear-scaling self-consistent implementation of the van der Waals density functional, Phys. Rev. B. 79 (2009), 201105.
[37] Y.W. Son, M.L. Cohen, S.G. Louie, Energy gaps in graphene nanoribbons, Phys. Rev. Lett. 97 (2006), 216803.
[38] S. Okada, A. Oshiyama, Magnetic ordering in hexagonally bonded sheets with first-row elements, Phys. Rev. Lett. 87 (2001), 146803.
[39] L. Brey, H.A. Fertig, Electronic states of graphene nanoribbons studied with the Dirac equation, Phys. Rev. B. 73 (2006), 235411.
[40] P.P. Shinde, J. Liu, T. Dienel, O. Gröning, T. Dumslaff, M. Mühlinghaus, A. Narita, K. Müllen, C.A. Pignedoli, R. Fasel, P. Ruffieux, D. Passerone, Graphene nanoribbons with mixed cove-cape-zigzag edge structure, Carbon 175 (2021) 50–59.
[41] H. Şahin, R.T. Senger, S. Ciraci, Spintronic properties of zigzag-edged triangular graphene flakes, J. Appl. Phys. 108 (2010), 074301.
[42] S. Song, J. Su, M. Telychko, J. Li, G. Li, Y. Li, C. Su, J. Wu, J. Lu, On-surface synthesis of graphene nanostructures with π-magnetism, Chem. Soc. Rev. 50 (2021) 3238–3262.
[43] L. Zhang, J. Chen, L. Zhang, F. Xu, L. Xiao, S. Jia, Gate controllable optical spin current generation in zigzag graphene nanoribbon, Carbon 173 (2021) 565–571.
[44] V. Barone, O. Hod, G.E. Scuseria, Electronic structure and stability of semiconducting graphene nanoribbons, Nano Lett. 6 (2006) 2748–2754.
[45] Z.F. Wang, Q. Li, H. Zheng, H. Ren, H. Su, Q.W. Shi, J. Chen, Tuning the electronic structure of graphene nanoribbons through chemical edge modification: a theoretical study, Phys. Rev. B. 75 (2007), 113406.
[46] E. Kan, Z. Li, J. Yang, J.G. Hou, Half-metallicity in edge-modified zigzag graphene nanoribbons, J. Am. Chem. Soc. 130 (2008) 4224–4225.
[47] Y.T. Zhang, H. Jiang, Q. Sun, X.C. Xie, Spin polarization and giant magnetoresistance effect induced by magnetization in zigzag graphene nanoribbons, Phys. Rev. B. 81 (2010), 165404.
[48] Z.F. Wang, F. Liu, Giant magnetoresistance in zigzag graphene nanoribbon, Appl. Phys. Lett. 99 (2011), 042110.
[49] D. Tománek, S.G. Louie, First-principles calculation of highly asymmetric structure in scanning-tunneling-microscopy images of graphite, Phys. Rev. B. 37 (1988) 8327–8336.
[50] F. Maier, J. Ristein, L. Ley, Electron affinity of plasma-hydrogenated and chemically oxidized diamond (100) surfaces, Phys. Rev. B. 64 (2001), 165411.